ADVANCED FUNCTIONAL MATERIALS
www.afm-journal.de

Evidence for Edge-State Photoluminescence in Graphene Quantum Dots

*Kiran Lingam, Ramakrishna Podila, Haijun Qian, Steven Serkiz, and Apparao M. Rao**

For a practical realization of graphene-based logic devices, the opening of a band gap in graphene is crucial and has proven challenging. To this end, several synthesis techniques, including unzipping of carbon nanotubes, chemical vapor deposition, and other bottom-up fabrication techniques have been pursued for the bulk production of graphene nanoribbons (GNRs) and graphene quantum dots (GQDs). However, only limited progress has been made towards a fundamental understanding of the origin of strong photoluminescence (PL) in GQDs. Here, it is experimentally shown that the PL is independent of the functionalization scheme of the GQDs. Following a series of annealing experiments designed to passivate the free edges, the PL in GQDs originates from edge-states, and an edge-passivation subsequent to synthesis quenches the PL. The results of PL studies of GNRs and carbon nano-onions are shown to be consistent with PL being generated at the edge sites of GQDs.

1. Introduction

Graphene has generated an enormous interest in carbon science and technology due to its unique properties,[1–3] for example, its high electron mobility of ≈10^6 cm^2 V^{-1} s^{-1} is very attractive for nanoelectronics.[4,5] However, for practical realization of graphene-based logic devices, opening of a band gap in graphene is crucial, a goal which has proved challenging. Previous reports indicate that the dimensions of graphene must be below 100 nm to facilitate an opening of a band gap in its otherwise semi-metallic band structure.[6–8] To this end, several synthesis techniques including unzipping of carbon nanotubes,[9,10] chemical vapor deposition[11] and other bottom-up fabrication techniques[12] have been pursued for the bulk production of graphene nanoribbons (GNRs) and graphene quantum dots (GQDs);[13–19] and only a limited progress has been made towards a fundamental understanding of the electronic and optical properties of GNRs and GQDs. In particular, the origin of strong photoluminescence (PL) in GQDs, which has been attributed to the presence of emissive surface traps[18] and/or the edge-states in GQD,[13,20] remains inconclusive to date. Previously, Pan et al. attributed the PL emission in GQDs to the triplet states from zig-zag edges,[13] but experimental evidence to support this claim remains uncompelling. We, therefore, have completed an in-depth study in an attempt to elucidate the origin of PL in GQDs. In this study, we have systematically varied the functionality and edge structure of the carbon nanostructures (GQDs, GNRs) using a combination of synthesis and annealing techniques to investigate the influence of structure on the observed PL. We found the PL of GQDs to be independent of suspension medium and the structure of its edges. As simple analogues to the carbon nanostructures, the PL spectra of benzene, anthracene, naphthalene, and pyrene were compared to data from GQDs, GNRs and carbon nano-onions (CNOs), and this comparison serves as a basis for future theoretical and experimental studies of PL in carbon nanostructures.

2. Results and Discussion

The transmission electron microscopy (TEM) studies of GQD samples (S1-DMF and S2-NaOH) prepared in this study exhibited a mean diameter ≈4 nm (**Figure 1**, see Experimental Section for details). The high-resolution TEM (HR-TEM) images of isolated GQDs (see, e.g., Figure 1b) confirmed the highly crystalline nature of our GQDs.

The presence of a strong π–π* transition peak (≈4.5 eV) in the UV-Visible spectrum further confirmed the sp^2 covalent bonding in our samples (Figure SI1, Supporting Information). Interestingly, the PL spectra for S1-DMF and S1-NaOH are very similar despite their synthesis in two different solvents (**Figure 2**). Consistent with previous studies,[14,19] both samples exhibited green luminescence at ≈510 nm with a broad full-width-at-half-maximum height (FWHM) of ≈90 nm upon excitation at 400 nm. In fact, S1-DMF and S2-NaOH showed

---

K. Lingam, R. Podila, Prof. A. M. Rao
Department of Physics and Astronomy
Clemson University
Clemson, SC 29634, USA
E-mail: arao@clemson.edu
H. Qian
Electron Microscope Facility
Clemson Research Park
Clemson University
Anderson, SC 29625, USA
S. Serkiz
Savannah River National Laboratory
Aiken, SC 29808, USA
A. M. Rao
Center for Optical Materials Science and Engineering Technologies
Clemson University
Clemson, SC 29634, USA

DOI: 10.1002/adfm.201203441

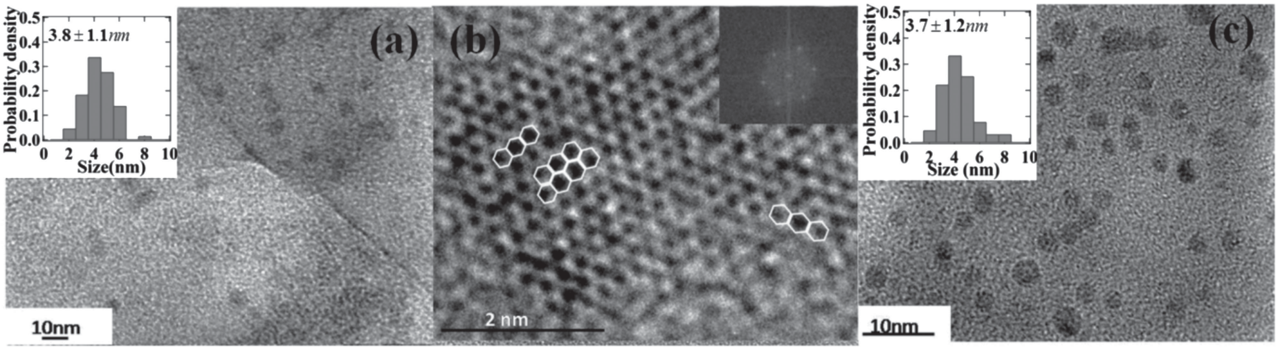

Figure 1. a) TEM and b) HR-TEM image of graphene quantum dots prepared using the solvothermal treatment in DMF (S1-DMF). The zigzag edges are marked as a guide to the eye and the inset in (b) shows the fast Fourier transform of the image. c) TEM image of GQD prepared via the hydrothermal treatment in NaOH (S2-NaOH). The insets in (a) and (c) show the diameter distributions of the corresponding samples.

similar shifts (upshift between 400–460 nm and negligible shift between 460–540 nm) in their peak emission wavelengths with increasing excitation wavelengths.

Although similar shifts in emission were previously observed in studies involving GQDs and other nanocarbons, a consensus regarding its origin is still lacking.[13,15,20] As shown in Figure SI2 (Supporting Information), a deconvolution of the PL spectrum of GQDs excited at 400, 440 or 480 nm, revealed the presence of at least three distinct Lorentzians, each with a FWHM of 40 ± 10 nm. Clearly, the peak positions of the deconvoluted traces for S1-DMF (Figure SI2a–c, Supporting Information) and S2-NaOH (Figure SI2d–f, Supporting Information) are similar to each other. Hence, the lack of a significant spectral difference for S1-DMF and S2-NaOH samples suggests that the presence of surface passivating functional groups (such as –OH groups in S2-NaOH or non-covalently coated DMF in S1-DMF), or other surface emissive traps bonded to GQDs are not the source for the observed PL in GQDs.

We further note that previous studies[17] on the PL of GQDs reported an upshift in emission wavelength by ≈90 nm for increasing excitation wavelengths. The dependence of the three deconvoluted peak positions (labeled 1, 2 and 3 in **Figure 3**a) on the excitation wavelength is significant for peak 1, as compared to peaks 2 and 3. In addition, a relative change in the intensities of these three peaks is evident with the second and third peaks becoming more prominent than the first peak with increasing excitation wavelength (Figure 3b). These findings underscore the need for a detailed analysis (Figure SI2, Supporting Information, and Figure 3) to determine the cause for the apparent ≈90 nm shift in the emission wavelength reported in previous studies.[13,14,20]

We next addressed the possibility that the edge-states in GQDs lead to the observed PL in GQDs via systematic annealing and passivating experiments. Previously, Xu et al. used micro-Raman spectroscopy to show that the graphene edges reconstruct upon annealing in vacuum.[21] Accordingly, to confirm the role of zig-zag edges in the PL of GQDs states as proposed by Pan et al.,[13] we vacuum annealed the S1-DMF sample and tracked the corresponding changes in its PL behavior when excited at 400 nm (**Figure 4**a). Prior to the vacuum annealing step, the GQDs were separated from the solution by evaporating the DMF. The as-obtained powder was annealed for 15 min at different temperatures under vacuum (≈1 mbar) and the final products were re-dispersed in DMF for PL measurements. The TEM and HR-TEM images (Figure 4) confirmed the presence of GQDs in the annealed sample. The PL spectrum of the annealed S1-DMF sample (vacuum annealed at 250 °C for 15 min) exhibited a significant drop in the intensity of its PL signal (Figure 4a). Interestingly, the other spectral features such as the excitation-dependent emission of the GQDs and the relative changes in the emission intensity as a function of excitation wavelength remained identical to that of the as-prepared sample (Figure SI3, Supporting Information). The PL intensity was observed to decrease further with increasing annealing temperature (Figure 4a,b). For comparison, we also recorded the emission for the annealed S1-DMF sample using the 460 nm excitation and found a decrease in the PL intensity with increasing annealing temperatures (Figure SI4, Supporting Information). We attribute this reduction in PL intensity to the possible rearrangement/passivation of edge

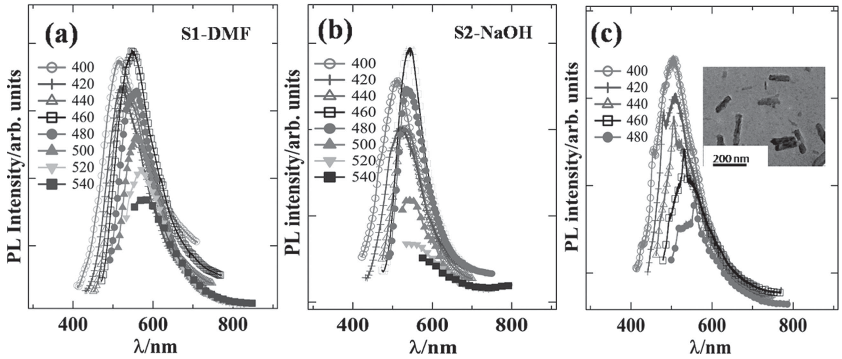

Figure 2. Photoluminescence spectra of graphene quantum dots as a function of excitation wavelength from 400 nm to 540 nm (with 20 nm increments) synthesized using solvothermal method in a) DMF and b) NaOH and c) for graphene nanoribbons suspended in DMF. The inset in (c) shows the TEM image of the GNRs sample.

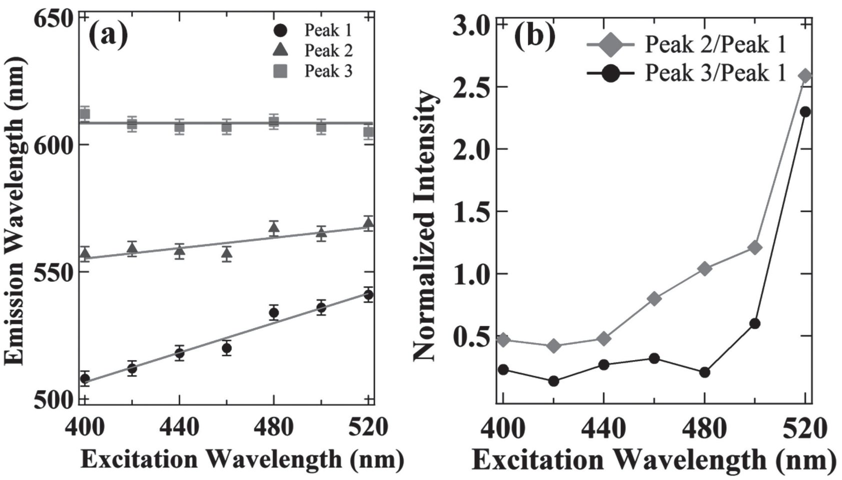

Figure 3. Plots of a) emission peak positions of S1-DMF sample as a function of excitation wavelength and b) the ratio of peak intensities with respect to peak 1.

carbon atoms in the GQDs. The HR-TEM images of isolated GQDs indicated the presence of disordered edges both before (Figure 1b) and after annealing (Figure 4e). Thus, the edge type appears randomized and implies that a preferred edge structure (armchair or zigzag) in the GQD is absent. This data appears to be inconsistent to the idea that the origin of PL is due to a particular edge type. In fact, Radovic et al.[22] showed that both the armchair and zigzag edges behave like carbene and carbyne sites respectively, both of which could lead to PL in GQDs.

In order to further investigate the passivation-induced reduction in the PL of GQDs: (i) we annealed the S1-DMF samples in H_2 atmosphere (rather than vacuum) at a relatively low temperature (250 °C). Interestingly, its emission was quenched upon excitation at 400 nm implying a correlation between the passivation of the edge-states and PL intensity (Figure 4c). Similar quenched emission behavior was observed in the hydrogen annealed sample when excited at 460 nm (Figure SI5, Supporting Information). (ii) We performed PL studies on GNRs possessing only a few layers with a uniform width of ≈25 nm and length ≈200 nm (inset in Figure 2c). The PL spectrum of these GNRs was strikingly similar to that of the GQDs with a nearly identical excitation-dependent emission profile (Figure 2c). The similarity in the PL spectra of GQDs and GNRs, despite the differences in their morphology and size, strongly suggested that the PL originates from the disordered edge-states. (iii) We extended our PL studies to CNOs which are cage-like structures made of a combination of hexagonal and pentagonal rings of carbon atoms. It is noteworthy that free edges are absent in CNOs due to their closed cage-like structure. As expected, we did not observe any PL signal for CNOs in agreement with the edge-state hypothesis (Figure SI6, Supporting Information). Collectively, the PL data for as-prepared, annealed GQDs, and as-prepared GNRs provide evidence that the disordered edges are responsible for the observed luminescence in these nanocarbons.

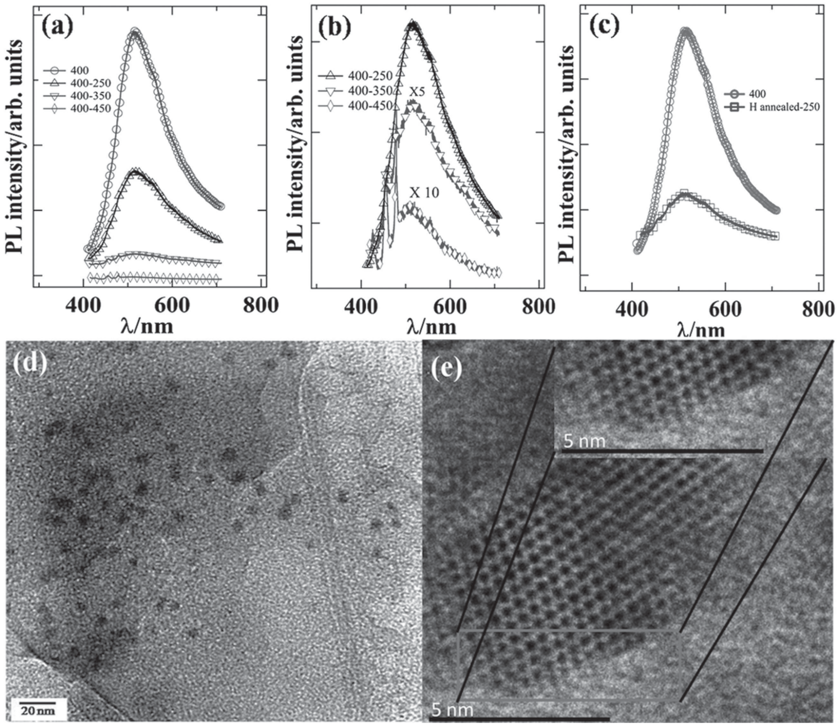

Figure 4. Panel (a) shows the change in the intensity of PL emission with 400 nm excitation as a function of annealing temperature; panel (b) shows the magnified view of the PL spectra of annealed samples, the sharp features correspond to the overtones of the excited light, and panel (c) shows the change in the intensity of PL emission with 400 nm excitation upon annealing in hydrogen atmosphere. The TEM and HRTEM images of GQDs post annealed at 450 °C are shown in (d) and (e), respectively. e) The graphitic nature of the annealed GQDs is evident, and the inset shows the presence of disordered edges in GQDs.

Lastly, we propose that GQDs may be viewed as a highly conjugated system of benzene rings with its emission peaks arising from HOMO-LUMO levels similar to that of poly-aromatic molecules. Previously, the PL in polyaromatic molecules has been attributed to the electronic transitions between the discrete HOMO-LUMO levels,[23,24] and it is well known that the PL profile of polyaromatic molecules red-shift in wavelength with increasing conjugation length (Figure SI7, Supporting Information). Further theoretical studies are needed to gain better understanding of PL behavior in GQDs.

3. Conclusions

In summary, we have investigated the origin of PL in GQDs. GQDs were prepared in two different solvents using similar techniques. The strikingly similar PL spectra of these samples suggest that the functional groups are not contributing to PL. Following a series of annealing experiments that resulted in GQDs with randomized edges, we observed that PL appears to originate from the edge-states of GQD, and edge passivation resulting from annealing leads to quenching of the PL signal. Furthermore, we studied the luminescent behavior in other nanocarbon systems such as GNRs with similar edge-states as GQDs and CNOs with a cage structure and no free edges to understand the results obtained for GQDs. GQDs and GNRs gave similar PL spectra while no PL spectra was detected in case of CNOs. Lastly, we propose that GQDs can be considered as highly conjugated benzene rings and the PL peaks (peaks 1, peak 2 and peak 3) observed can be attributed to electronic transition between HOMO-LUMO levels.

4. Experimental Section

GQDs used in the present study were synthesized using a modified version of a previously reported solvothermal method.[14] GQD samples were prepared by mixing ≈200 mg of as-purchased graphene nanoplatelets (GNPs; XG Science, grade-M, 8 μm wide and 5–8 nm thick) with 40 mL dimethylformamide (DMF) (Alfa Aesar) and tip sonicating (power ≈40 W) for 30 min before transferring the dispersion into a Teflon®- lined autoclave. The GQDs, hereafter referred as S1-DMF, were obtained following a heating step for 5 h at 200 °C and subsequently collected by filtration through a 0.22 μm Teflon membrane. Another batch of GQDs (S2-NaOH) was prepared using an identical procedure in NaOH diluted in DI water to a pH = 9. Since, DMF and NaOH are two completely different solvents, during the synthesis process, they form different functional groups with GQDs. PL measurements on such samples help in understanding the role of functional groups.

The GQDs were characterized using a high resolution Hitachi TM 9500 transmission electron microscope (HR-TEM) operated at 300 kV. GQD solution was drop casted onto TEM grids for analysis.

A double grating Horiba Jobin Yvon spectrometer equipped with liquid nitrogen cooled CCD was used for recording the room temperature PL data, equal volume of samples were used for all the measurements in a quartz cuvette.

Graphene nanoribbons (GNRs) used in this study were produced by filtering the dispersion of the as-purchased GNPs in DMF through a 0.2 μm Teflon membrane. Carbon nano-onions were produced from the arc-discharge method.[25] GNRs and CNOs were characterized using TEM and PL as described above for the GQDs.

Supporting Information

Supporting Information is available from the Wiley Online Library or from the author.

Acknowledgements

The authors gratefully acknowledge the financial support from SCUREF and would like to thank Dr. Malcolm Skove at the Physics Department at Clemson University for his valuable inputs.

Received: November 22, 2012
Revised: February 5, 2013

[1] K. S. Novoselov, A. K. Geim, S. V. Morozov, D. Jiang, Y. Zhang, S. V. Dubonos, I. V. Grigorieva, A. A. Firsov, *Science* **2004**, *306*, 666.
[2] A. K. Geim, K. S. Novoselov, *Nat. Mater.* **2007**, *6*, 183.
[3] A. K. Geim, *Science* **2009**, *324*, 1530.
[4] M. C. Lemme, T. J. Echtermeyer, M. Baus, H. Kurz, *IEEE Electron Device Lett.* **2007**, *28*, 282.
[5] M. Y. Han, B. Özyilmaz, Y. Zhang, P. Kim, *Phys. Rev. Lett.* **2007**, *98*, 206805.
[6] Y.-W. Son, M. L. Cohen, S. G. Louie, *Phys. Rev. Lett.* **2006**, *97*, 216803.
[7] V. Barone, O. Hod, G. E. Scuseria, *Nano Lett.* **2006**, *6*, 2748.
[8] L. Yang, C.-H. Park, Y.-W. Son, M. L. Cohen, S. G. Louie, *Phys. Rev. Lett.* **2007**, *99*, 186801.
[9] D. V. Kosynkin, A. L. Higginbotham, A. Sinitskii, J. R. Lomeda, A. Dimiev, B. K. Price, J. M. Tour, *Nature* **2009**, *458*, 872.
[10] L. Jiao, L. Zhang, X. Wang, G. Diankov, H. Dai, *Nature* **2009**, *458*, 877.
[11] J. Campos-Delgado, J. M. Romo-Herrera, X. Jia, D. A. Cullen, H. Muramatsu, Y. A. Kim, T. Hayashi, Z. Ren, D. J. Smith, Y. Okuno, T. Ohba, H. Kanoh, K. Kaneko, M. Endo, H. Terrones, M. S. Dresselhaus, M. Terrones, *Nano Lett.* **2008**, *8*, 2773.
[12] J. Cai, P. Ruffieux, R. Jaafar, M. Bieri, T. Braun, S. Blankenburg, M. Muoth, A. P. Seitsonen, M. Saleh, X. Feng, K. Mullen, R. Fasel, *Nature* **2010**, *466*, 470.
[13] D. Pan, J. Zhang, Z. Li, M. Wu, *Adv. Mater.* **2010**, *22*, 734.
[14] S. Zhu, J. Zhang, C. Qiao, S. Tang, Y. Li, W. Yuan, B. Li, L. Tian, F. Liu, R. Hu, H. Gao, H. Wei, H. Zhang, H. Sun, B. Yang, *Chem. Commun.* **2011**, *47*, 6858.
[15] Y. Dong, C. Chen, X. Zheng, L. Gao, Z. Cui, H. Yang, C. Guo, Y. Chi, C. M. Li, *J. Mater. Chem.* **2012**, *22*, 8764.
[16] R. Liu, D. Wu, X. Feng, K. Müllen, *J. Am. Chem. Soc.* **2011**, *133*, 15221.
[17] J. Shen, Y. Zhu, X. Yang, C. Li, *Chem. Commun.* **2012**, *48*, 3686.
[18] S. Zhu, J. Zhang, X. Liu, B. Li, X. Wang, S. Tang, Q. Meng, Y. Li, C. Shi, R. Hu, B. Yang, *RSC Adv.* **2012**, *2*, 2717.
[19] D. Pan, L. Guo, J. Zhang, C. Xi, Q. Xue, H. Huang, J. Li, Z. Zhang, W. Yu, Z. Chen, Z. Li, M. Wu, *J. Mater. Chem.* **2012**, *22*, 3314.
[20] J. Peng, W. Gao, B. K. Gupta, Z. Liu, R. Romero-Aburto, L. Ge, L. Song, L. B. Alemany, X. Zhan, G. Gao, S. A. Vithayathil, B. A. Kaipparettu, A. A. Marti, T. Hayashi, J.-J. Zhu, P. M. Ajayan, *Nano Lett.* **2012**, *12*, 844.
[21] Y. N. Xu, D. Zhan, L. Liu, H. Suo, Z. H. Ni, T. T. Nguyen, C. Zhao, Z. X. Shen, *ACS Nano* **2010**, *5*, 147.
[22] L. R. Radovic, B. Bockrath, *J. Am. Chem. Soc.* **2005**, *127*, 5917.
[23] M. Fox, *Optical Properties of Solids*, vol. *1*, Oxford University Press, New York **2010**, p. 227.
[24] M. Mueller, X. Yan, J. A. McGuire, L. S. Li, *Nano Letters* **2010**, *10*, 2679.
[25] M. K. Sreeramoju, J. P. Selegue, in *Proc. Carbon Conf.* Omnibooks, Clemson, SC, USA **2010**.